frontiers | Frontiers in Earth Science

TYPE Original Research
PUBLISHED 21 March 2025
DOI 10.3389/feart.2025.1522361

OPEN ACCESS

EDITED BY
Jiangyu Wu,
China University of Mining and Technology, China

REVIEWED BY
Mehmet Kaya,
Bozok University, Türkiye
Jiewen Pang,
Taiyuan University of Science and Technology, China
Jinlong Zhou,
China Coal Research Institute, China

*CORRESPONDENCE
Zewei Li,
15651465083@163.com

RECEIVED 04 November 2024
ACCEPTED 12 February 2025
PUBLISHED 21 March 2025

CITATION
Wang F, Li Z, Shi Y, Gong X and Zhang Y (2025) Microstructure analysis and mechanical parameter estimation of sanding dolomite. *Front. Earth Sci.* 13:1522361. doi: 10.3389/feart.2025.1522361

Microstructure analysis and mechanical parameter estimation of sanding dolomite

Fengnian Wang[1,2,3,4], Zewei Li[1,4]*, Yongxiang Shi[1,4], Xiaowen Gong[5] and Yanjie Zhang[5]

[1]Shanxi Traffic Technology Research and Development Co., LTD., Taiyuan, China, [2]State Key Laboratory for Tunnel Engineering, China University of Mining and Technology-Beijing, Beijing, China, [3]School of Earth Sciences and Engineering, Hohai University, Nanjing, China, [4]Shanxi Intelligent Transportation Laboratory Co., LTD., Taiyuan, China, [5]Yunnan Dianzhong Water Diversion Engineering Co., LTD., Kunming, China

Sanding dolomite strata are widely distributed in southwest China. The safety of the water diversion tunnel in Yuxi section of the Central Yunnan water diversion Project has been seriously threatened by the geological disasters such as the reduction of rock strength caused by dolomite sanding and tunnel sand inrush. In order to explore the mechanical characteristics and obtain the mechanical parameters of sanding dolomite quickly and accurately, this study relies on the Central Yunnan Water diversion Project to first established the classification standard of dolomite sanding grade. The pore structure, microscopic composition and morphological distribution of dolomite with different sanding degrees were studied by means of SEM scanning, EDS spectroscopy and CT scanning. At the same time, based on the field needle penetration test and the Hoek-Brown strength criterion considering the wave velocity and integrity coefficient of rock mass, a method for estimating the mechanical parameters of sanded dolomite was proposed, which was verified by NPI test and field adit test. The results showed that the sanding dolomite could be divided into four grades: slight sanding dolomite, moderate sanding dolomite, strong sanding dolomite and severe sanding dolomite. The higher the sanding grade, the higher the development degree of dolomite pores and the lower the mechanical strength. The action of groundwater will aggravate the dolomite dissolution sanding and lead to the aggravation of surrounding rock breakage. Based on the improved Hoek-Brown strength criterion, the cohesion of strong sanding dolomite is 0.34~0.71 MPa, the internal friction Angle is 38.59~50.96°, the uniaxial compressive strength is 3~15.41 MPa, and the cohesion of severe sanding dolomite is 0.086~0.17 MPa, the internal friction Angle is 16.17~19.08°, the uniaxial compressive strength is 0.88–1.67 MPa. And the results were basically consistent with those of needle penetration test and dynamic rock mass tunnel test.

KEYWORDS

Sanding, dolomite, microstructure, mechanical parameters, estimate, test

1 Introduction

In the process of tunnel construction in the southwest of China, many bad geological problems have been encountered, and the Sandification of dolomite phenomenon is

a typical one (Wang et al., 2019). Sandification of dolomite refers to a special karst geological phenomenon in which the dolomite with microcrystalline and fine crystalline structure is weathered into fine sand, gravel, or fragments due to the combined effects of dissolution and weathering in a complex geological environment, resulting in a significant decrease in the overall strength of the rock mass.Sanding dolomite is the product of Sandification of dolomite strata. Its rock mass engineering characteristics show that its strength is reduced, a large number of pores are formed, and it can be squeezed into sand by hand. After disturbance, it is easy to loose and become a mixture of sand and powder, and it is easy to produce permeability deformation under osmotic pressure, resulting in water inrush sand phenomenon. "Sanding" of dolomite is a very special geological phenomenon, which is obviously different from the general weathered rock mass. The geological bodies are manifested as volumetric loosening and fragmentation, and are also different from the differential weathering and interlayer weathering in weathered rock formations (Wu et al., 2017; Cui et al., 2015; Zhou et al., 2022). The strength of sanding dolomite rock mass deteriorates and the quality of rock mass decreases, especially in the rich water tunnel section, it is easy to produce secondary geological disasters such as gusher (flowing) sand and debris flow in the tunnel, which leads to slow project progress, increased safety problems and increased investment. Therefore, it is necessary to study the microstructure and surrounding rock stability of dolomite with different degrees of sanding (Li et al., 2018; Wu et al., 2021; Yang et al., 2019).

The formation mechanism and structural characteristics of sanding dolomite have been studied by many scholars. Masaharu et al. (2011) believed that dolomite wouldl be produced when Mg/Ca ratio was 0.5, but after a long time, microbial action would induce the formation of dolomite sandification. Richter et al. (2018) took 8 surface outoutings of Jurassic dolomites in Bavaria, southeast Germany, as examples, and combined with relevant theory of cathodoluminescence technology, scanning electron microscopy, petrography and geochemistry, proposed the evolution process of dolomitization. Sajjad et al. (2020), Wu et al. (2022) revealed the dolomite sanding phenomenon of the Lower Cretaceous in the deposit in the southern Yazd Basin, Iran, which existed only near the normal fault as the main channel of ore-forming fluid, and believed that dolomite sanding into hydrothermal process occurred there. Jiang et al. (2023) compared and analyzed the differences between dolomite and limestone karst. It was believed that the porosity of dolomite was higher than that of limestone, which could provide a better channel for surface water and groundwater, and it was easier to form the shedding of dolomite crystals and the formation of weathering products dispersed by dolomite sand. Wang et al. (2021), Guo et al. (2014), Dong et al. (2023) and Chen et al. (2022) showed through the laboratory dissolution test of dolomite and the study on the mechanism of microscopic dissolution that the characteristics of microscopic dissolution of dolomite mainly showed that under chemical action, all kinds of joints and cracks inside dolomite crystals were dissolved first, and the strength of intercrystal bonding was reduced. Under the physical action of water flow, mechanical disintegration and fall off occurred, and eventually formed dolomite sand (powder) like material. Liu et al. (2022) believed that the formation mechanism of the "dissolution" phenomenon of fine-grained dolomite was that water circulates in the pores of rocks, dissolved the cementing calcite first, increased the porosity and decreases the strength of rocks, and finally leaved loose dolomite powder. Zhang et al. (2012) proposed three formation mechanisms of dolomite powder in microscopic state, namely, dissolution of embedded structure, permeation-dissolution decomposition, mechanical disintegration and dissolution.By analyzing the mineral composition and karst characteristics of dolomite, Dong et al. (2024), Zhang (2025) and Zhu et al. (2024a), Zhu et al. (2024b) believed that the formation mechanism of dolomite sanitization was mainly the dissolution failure of Mosaic structure. The calcite veins in dolomite were preferred to dissolve, the rock mass was broken into rock fragments, and the Mosaic structure of the rock was dissolved and thus decomposed into sanded dolomite with different degrees of sanitization. Weng (1984),Yan et al. (2007), Yin et al. (2023a), Yin et al. (2023b) believed that the formation mechanism of dolomitization was mainly penetration-solution-decomposition and mechanical disintegration failure, and the dolomites dissolved and disintegrated along the intercrystal void or crystal bonding surface, during which the crystals fell off to form sanded dolomites with different degrees of sanitization.

To obtain mechanical parameters of dolomite, Zhao (2021) used indirect splitting method to study the tensile strength of dolomite with different sanded degrees. Tian and Yue (2014) studied the rock mass mechanical parameters of dolomite under different karst sanding conditions through laboratory tests. Wu (2021) made standard rock samples by reshaping sanding dolomite, carried out triaxial compression test, and studied mechanical parameters of sanded dolomite with different particle content. Dong et al. (2022) estimated the mechanical parameters of rock mass based on the Hoek-Brown strength criterion, and compared the estimated results with the results of *in-situ* rock mass adit test. The results showed that the Hoek-Brown strength criterion was effectively applied in the estimation of mechanical parameters of strongly sanded dolomite rock mass.

To sum up, dolomite sanding is a common bad geological condition. Engineering construction in this area will not only reduce the engineering strength of rock mass, cause slope collapse, debris flow, tunnel sand influx, etc., but also lead to prevention difficulties, slow progress of the project, resulting in major safety accidents. At the same time, the genesis, properties and parameter determination of sanded dolomite are not clear at present. Therefore, it is very important to study the engineering micro-mechanism and engineering characteristics of sanded dolomite. Although some researches on dolomitization have been carried out by predecessors (Wu et al., 2024; Wu et al., 2020), most of them remain in the description and theoretical analysis of macro phenomena, and the researches on the microstructure of dolomitization with different degrees of sandification are relatively lacking. Meanwhile, the difficulty of making standard rock samples for laboratory tests to obtain rock mechanics parameters has not been solved in view of the structure fragmentation and joint development of dolomitization rock mass. Therefore, in this paper, the sanding dolomites along the Yuxi section tunnel of the Central Yunnan water diversion Project were taken as the geological background. On the basis of previous studies, the microscopic composition and morphological distribution of the dolomites with different sanding degrees were studied by SEM electron microscope and EDS spectrum test, and the pore structure of the dolomites with different sandeing degrees

was studied by CT. At the same time, based on the field needle penetration test and the Hoek-Brown strength criterion considering rock wave velocity and integrity coefficient, a method for estimating the mechanical parameters of sanded dolomite was proposed, and the estimated results were compared with the field rock tunnel test results, which could provide a reference for the engineering construction of sanded dolomite formation.

2 Classification of dolomite sanding

The classification of surrounding rock of tunnel is the foundation and key to evaluate the stability of surrounding rock, and the accuracy of classification is directly related to the subsequent design, excavation and support. At present, the classification of dolomite sandification is mainly characterized by qualitative description, or by a single index or a variety of indexes. According to the research of Wu et al. (2022) the dolostones in Yuxi Section are macroscopically divided into four grades of severe sanding, strong sanding, modera.e sanding, and slight sanding. Typical photos of dolomite with different sanding grade are shown in Figure 1. However, through field investigation, it is found that the degree of dolomite sanding in the study area is not uniform, and various indexes vary with the degree of sanding, and several indexes often contradict each other. Based on the macroscopic classification of dolomite sanding, this paper takes into account the quantitative indexes such as rock integrity coefficient Kv, resilience index Rm, point load index Is(50), and injection index NPI, and introduces analytic hierarchy process (AHP) and fuzzy comprehensive evaluation methods to classify dolomite sanding grades in a targeted, targeted and practical way from the Angle of qualitative and quantitative combination.

2.1 Selection principle of classification index

(1) The principle of importance. By studying the engineering geological characteristics and physical and mechanical characteristics of the sanding dolomite in the study area, this study selected some indexes that can best reflect the change of the sanded degree of the dolomite, so that the evaluation index system can reflect the sanded status of the dolomite in the study area more accurately.

(2) The principle of hierarchy. In this study, the selection of evaluation criteria reflects the characteristics of structure and order. We classify these standards reasonably according to the established principles, so as to facilitate the comparative analysis of similar types of standards. This method enhances the accurate evaluation of the importance of each evaluation indicator and makes their weight assignment more reliable and effective.

(3) Operability principle. In this study, the evaluation criteria adopted not only distinguish clearly, but also greatly improve the accessibility and economy. This characteristic makes the analysis process of the index more rapid, so as to effectively classify the dolomite sanding grade in the study area. This provides a reference for practical engineering design and construction.

2.2 Selection and basis of classification indicators

According to the existing weathering classification method of rock mass and considering the engineering characteristics of dolomite sanding in the study area, this study mainly selects 15 main indexes from the three aspects of the external characteristics, the structural characteristics of the rock mass and the physical and mechanical indexes of the sanding rock mass to classify the dolomite sanding grade.

The reasons for selecting classification indicators are as follows:

(1) External characteristics of sanding rock mass

This category of indicators focuses on observable features of the rock surface, such as color changes, water-rich environments, and particle size. The reason for choosing these indexes is that they can directly reflect the initial degree and external performance of rock mass sanding. These external features are usually the most direct and easily observed manifestations of sanding and can provide the basis for the preliminary assessment of rock sanding. For example, particle size can directly indicate the degree of weathering of a rock structure, while color changes can indicate changes in chemical composition.

(2) Structural characteristics of the rock mass

These indicators relate to structural changes within the rock, such as the number of joints per unit volume, the degree of structural plane development, and the size of the block. The selection of such indexes is based on the theory that the internal structure of rock mass directly affects its engineering characteristics, including stability and bearing capacity. Changes in internal structural characteristics often predict the depth of sanding, and these changes are crucial in engineering applications, because they affect the actual performance and treatment methods of rock mass in engineering.

(3) Physical and mechanical indexes

This includes the physical and mechanical properties of the rock, such as density, strength, and elastic modulus. These indexes are chosen because they can quantify the mechanical properties of rock, which is essential for understanding and predicting the behavior of rock mass in practical engineering. The physical and mechanical indexes can reflect the loss of strength, the change of density and the change of other mechanical properties of rock in the process of sanding, which directly affect the safety and applicability of rock in construction, excavation and support engineering applications.

The specific classification indicators are shown in Figure 2 and Table 1.

2.3 Weight allocation of influencing factors

According to the importance of the above evaluation indicators and the difficulty of obtaining them, AHP is used to determine the weights of the primary evaluation criteria and the secondary evaluation indicators. The comprehensive weights of the evaluation indicators of dolomite sanding are shown in Table 2.

FIGURE 1
Typical photos of dolomite with different sanding grade **(a)** slight sanding dolomite, **(b)** moderate sanding dolomite, **(c)** strong sanding dolomite, **(d)** severe sanding dolomite.

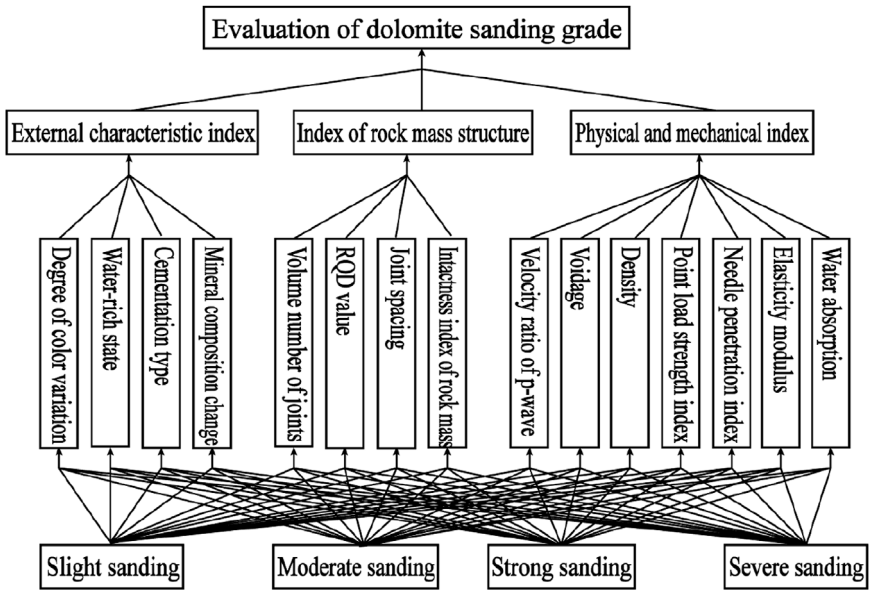

FIGURE 2
Evaluation system of dolomite sanding grade.

TABLE 1 Classification standard of sanding grade.

Evaluation index	Standard value of evaluation index			
	Slight sanding	Moderate sanding	Strong sanding	Severe sanding
degree of color variation	1 (fresh color)	2 (surface discolored mostly, fracture is fresh)	3 (surface and fracture discolor mostly)	4(Almost all discolor and dull)
moisture content (%)	1–3	4–6	7–8.5	>8.5
cementation type	structure is intact and cracks are closed	most cataclastic structure,a little mosaic structure, fragmentary granular structure	the structure is damaged, showing discontinuous skeleton, a little disintegrates into sand granular, weathered cracks develop, and contains a large number of secondary mud	the structure is completely destroyed and has disintegrated into loose sand particles with large volume changes
degree of change in mineral composition	the content of debris and spherules 20%, quartz 10%±	the content of dolomite 95%±, quartz content ≤5%, hydromica content 2%±	the content of algal mass 80%±, lake dolomite 10%, sparry dolomite 5%–10%, a small amount of quartz	the content of silica 80%±, dolomite content 20%±, a small amount of secondary quartz
volume number of joint	1–2	2–3	>3	—
RQD value (%)	>50	20–50	<20	—
joint spacing(m)	>1	0.4–1	0.2–0.4	<0.2
intactness index of rock mass	>0.5	0.25–0.5	0.1–0.25	<0.1
velocity of p-wave (km/s)	>4.15	2.55–4.15	1–2.55	<1
voidage	<0.05	0.5–0.12	0.12–0.20	>0.20
density (g/cm^3)	2.52–2.87	2.23–2.35	1.89–1.92	1.35–1.37
point load strength index (MPa)	>3.6	1.84–3.6	0.84–1.84	<0.84
needle penetration index (N/mm)	—	>40	15–40	<15
elasticity modulus (MPa)	>50	40–50	20–40	<20
water absorption	1 (almost no water absorption)	2 (surface flaked slightly after soaking)	3 (can be broken apart by hand after soaking)	4 (can be kneaded into a ball after soaking)

3 Microstructure of sanding dolomite

3.1 EDS spectrum test

The chemical composition and mineral content of rock samples have important guiding significance for the systematic understanding of the sanding of dolomite. In order to determine the mineral composition of dolomite of different degrees, EDS spectrum test was carried out on four kinds of sanding grades. The result was shown in Figure 3. The counting peaks of C, O, Mg, Ca, Al, Si, K and Fe appear in the samples of strong sanding dolomite, while the counting peaks of C, O, Mg, Si, Nb, Ca and Fe appear in the samples of severe sanding dolomite, and Ca:Mg changes from 1:0.57 to 1:0.67, indicating that the migration rate of Ca element is faster than that of Mg in the process of dolomite sanding. Table 3 shows the elemental weight percentage and atomic percentage of the dolomite of the two sanding grades. The weight and atomic percentage of Si elements in the severe sanding dolomite are much higher than those in the strong sanding dolomite, and the contents of Fe, Mg and Ca elements have not changed much, which is similar to the process of Si enrichment and Fe concentration in the dolomite under karst. Table 4 summarizes the occurrence frequency of each element in the 30 energy spectrum images, from high to low, they are C, O, Ca, Mg, Si, Fe, Al, Ti, K, Nb, Cl, Au, and rare earth elements do not appear. The frequency of C:O:Ca:Mg is about 1:1:0.89. From the analysis of element occurrence frequency, it can be seen that sanding dolomite is mainly composed of dolomite, and minerals containing Si, Fe, Al and other elements are produced or enriched in the evolution process. The mineral element composition of strong sanding dolomite and severe sanding dolomite is high Ca

TABLE 2 Comprehensive weight of evaluation index of dolomite sanding.

Primary evaluation index	Weight	Secondary evaluation index	Weight
external characteristic index	0.31	degree of color variation	0.2344
		moisture content (%)	0.2752
		cementation type	0.1978
		degree of change in mineral composition	0.2926
index of rock mass structure	0.23	volume number of joint	0.2025
		RQD value	0.2759
		joint spacing	0.1200
		intactness index of rock mass	0.2342
		velocity ratio of p-wave	0.1674
physical and mechanical index	0.46	voidage	0.1223
		density	0.1021
		point load strength index	0.1890
		needle penetration index	0.1512
		elasticity modulus	0.2622
		water absorption	0.1732

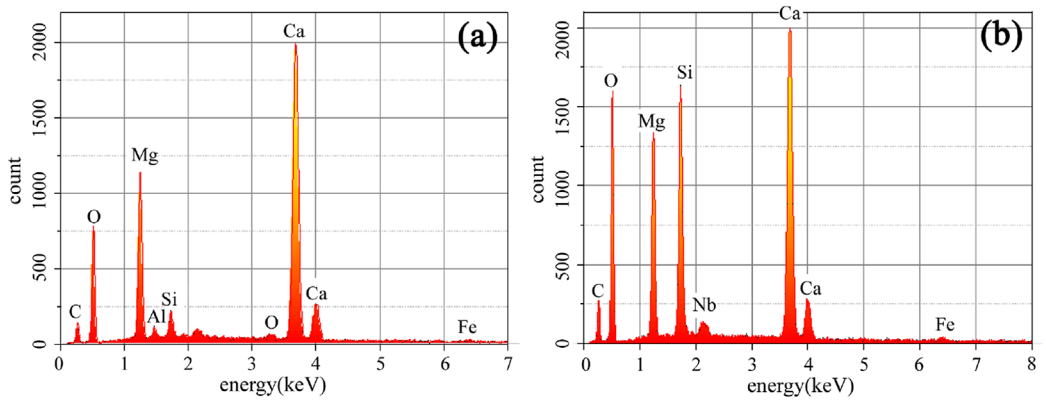

FIGURE 3
EDS images of dolomite with different degrees of sanding (30 kV) **(a)** strong sanding dolomite, **(b)** severe sanding dolomite.

and relatively low Mg, which indicates that dolomitization is not thorough, and may be related to the infiltration and backflow of pore water in the dolomite.

3.2 Scanning electron microscope test

The structure and *in situ* chemical composition of rock samples with thickness of 2 cm × 2 cm were analyzed by using field emission scanning electron microscopy. It can be seen from the rock surface morphological characteristics of the dolomite with different sanding degrees magnified by 2000 times in Figure 4 that a large number of blocky dolomite are closely arranged on the surface of slight sanding dolomite, with a good overall degree of dolomite, low degree of pore development, and a little particle disintegration and scattering. The surface of moderate sanding dolomite is broken into irregular particles, the amount of blocky dolomite is reduced, and a certain amount of solution pores are produced, without

TABLE 3 Results of spectrum analysis of dolomite with different sanding degrees.

Element	Strong sanding dolomite		Severe sanding dolomite	
	Weight percentage (%)	Atom percentage (%)	Weight percentage (%)	Atom percentage (%)
C	6.11	10.10	8.73	13.67
O	50.46	62.61	53.63	63.06
Mg	13.86	13.36	11.52	8.92
Al	0.94	0.69	0.00	0.00
Si	2.10	1.49	10.64	7.13
Ca	22.91	11.35	15.15	7.11
Fe	0.30	0.11	0.33	0.11

TABLE 4 Occurrence frequency of energy spectrum elements in sanding dolomite.

degree of sanding	Element and frequency											
	C	O	Ca	Mg	Si	Fe	Al	K	Nb	Ti	Cl	Au
moderate sanding, strong sanding, severe sanding	27	27	27	24	15	7	9	5	3	2	1	4

obvious grain structure. The surface fragmentation degree of strong sanding dolomite is intensified, a small amount of blocky dolomite can be seen, the number of dissolved pores is increased, and the small particles and dolomite particles cemented each other In the late cementation. There are traces of crystal expansion visible on the surface of the severe sanding dolomite. The content of blocky dolomite is very small, and the dolomite crystals all dissolve and fall off to form small particles, and there are a large number of solution pores.

At the same time, dolomite grains are distributed on the structural plane of dolomite with different sanding degrees, mostly square and rectangular structure, uneven size distribution, and pores and cracks are developed. With the increase of dolomite sandification degree, the decomposition degree of dolomite crystal increases, and the dissolution and loss of CaO in dolomite crystal increase, resulting in the decrease of Ca content and the increase of Mg content. It is preliminarily analyzed that dolomite crystals and other fine-grained minerals fall off under the action of internal and external forces, and dolomite sand, dolomite powder and fine-grained dolomite minerals are produced on a macro level.

In general, the microcosmic development of dolomites with different sanding degrees is quite different. With the increase of sanding grade, the interaction force between the dolomite rock layers decreases, the cementation effect decreases, the mechanical strength decreases, the surface of the dolomite forms a solution hole, more particles are formed, the cementation between the crystals decreases, there is obvious crystal expansion traces under the action of fluid, and finally the dissolution of small particles in bulk. Under the action of groundwater, it is easier to form through the water inrush channel, resulting in geological disasters.

3.3 Casting thin section test

Casting thin section test of dolomites with different sanding degrees was carried out, and the test results are shown in Figure 5. It can be seen that the dolomite gradually expands from micro cracks until it breaks, and the particle size gradually becomes smaller, resulting in the increase of the degree of dolomite sanding. The slightly sanding dolomite is crystalline dolomite with a particle size of 120–200um. The crystals are embedded with each other, the effective pores are not developed, and a few micro-cracks are developed. The moderate sanding dolomite is algal dolomite, which is distributed in clumping form, and the pores are filled with dolomite, some of the pores are formed by dissolution, and the intercrystalline voids and micro-cracks are developed.The strong sanding dolomite is algal dolomite, and between the pores are filled by two stages of dolomite, the early stage is powdery, the late stage is fine-grained, medium-grained or megachrystalline dolomite. The severe sanding dolomite is a clastic dolomite with a diameter of 0.5~2 mm. The impurities are mainly argillaceous and silty, and the gravel is fractured.

In addition, when the development of fracture pores was tested, it was found that the degree of pore development of dolomite showed an increasing trend with the increase of sanding grade. Among them, the mesoporous pores diameter of slight sanding dolomite was mainly distributed in the range of 2–10 nm, and the maximum pore volume was 2.4×10^{-5} cm3/nm. The diameter of macropore pores were mainly distributed in the range of 50–1,000 nm, with large void volumes mostly 0.001 cm^3/nm and maximum pore volumes 0.0021 cm^3/nm. The mesoporous pores diameter of moderate sanding dolomite was mainly distributed

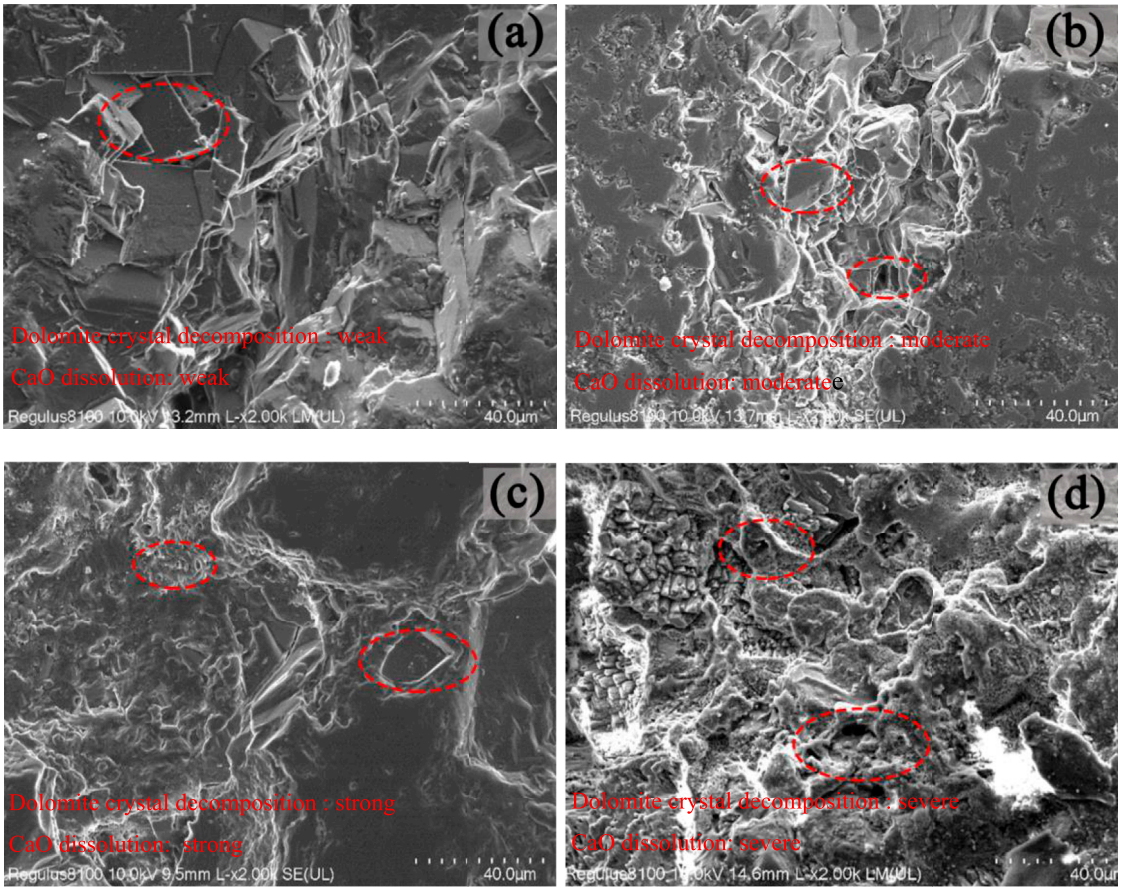

FIGURE 4
SEM images of dolomite with different sanding degrees **(a)** slight sanding dolomite, **(b)** moderate sanding dolomite, **(c)** strong sanding dolomite, **(d)** severe sanding dolomite.

in the range of 2–10 nm, and the maximum pore volume was 9.76×10^{-5} cm^3/nm. The diameter of macropores pore was mainly distributed in the range of 50–1,000 nm, with large void volumes mostly 0.01 cm^3/nm and maximum pore volumes 0.03 cm^3/nm. The mesoporous pores diameter of strong sanding dolomite was mainly distributed in the range of 2–10 nm, and the maximum pore volume was 9.32×10^{-4} cm^3/nm. The diameter of macropore pores were mainly distributed in 100–1,000 nm, and the macropore volume is linearly correlated with that of macropore pores, with a maximum pore volume of 0.17 cm^3/nm. The mesoporous pores diameter of the severe sanding dolomite was mainly distributed in the range of 2–10 nm, and the maximum pore volume was 5.76×10^{-3} cm^3/nm. The diameter of macropore pores were mainly distributed in the range of 500–1,000 nm, with a maximum pore volume of 0.35 cm^3/nm. The results of pore structure of dolomite with different sanding grades are shown in Figure 6.

3.4 CT test

SEM test only analyzed the surface microstructure of rock samples, and CT scanning test was carried out to further analyze the pore structure characteristics of dolomite with different degrees of sanding, and the results are shown in Figure 7. Red indicates the internal particles of the dolomite, blue indicates the development of pores and cracks in it, and green indicates complete minerals such as dolomite. The proportion of blue and red in the slight slight dolomite is small, and the proportion of green is very large, and the blue and red are scattered around the green, which indicates that the rock skeleton in the dolomite is complete, there are a few particles, and a few cracks are developed, and there is a tendency to form a fracture network. The proportion of blue in the moderate sanded dolomite increases greatly, while the proportion of red and green decreases, indicating that the integrity of the rock skeleton in the dolomite is damaged to a certain extent, the content of cracked particles increases slightly, the development of cracks is intensified, the cracks are connected with each other, and the fracture network is initially formed. The proportion of blue and green in strong sanding dolomite is greatly reduced, but the proportion of red is greatly increased, indicating that the integrity of rock skeleton inside dolomite is greatly damaged, and the content of cracked particles is greatly increased. Under cementation, small particles and dolomite particles cement each other, so the relative arrangement of particles is tight, temporarily covering the surface of pore cracks. As a result, the proportion of blue is reduced, but cracks and pore networks still develop together between particles. The proportion of blue in the

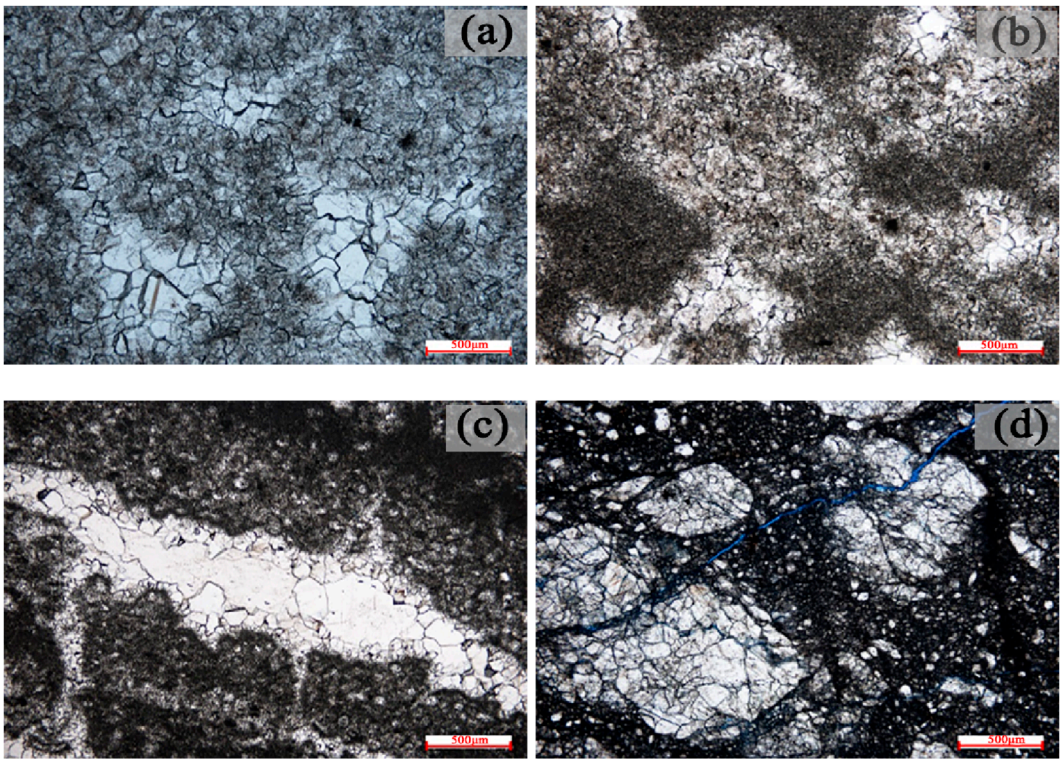

FIGURE 5
Results of dolomite cast thin sections with different sanding grades **(a)** slight sanding dolomite, **(b)** moderate sanding dolomite, **(c)** strong sanding dolomite, **(d)** severe sanding dolomite.

severe sanding dolomite increases significantly, while the proportion of green is very small, and the red part is dispersed and relatively reduced, indicating that there is almost no complete rock skeleton in the dolomite, and the dolomite is cracked into granular fragments, and the cementing force between particles decreases, resulting in the dispersed distribution of granular fragments, highly developed fracture network, and a large number of holes are formed.

From the above analysis, it can be seen that the microstructure of dolomite with different sanding degrees differs greatly, mainly in the degree of pore development. The higher the sanding grade, the more intense the degree of pore development. It can be inferred that the more serious the sanding, the more severe the fracture development. After the dolomite is dissolved by water, the surrounding rock will be more broken, and then the original layer cracks and structural cracks in the surrounding rock will continue to expand, thus creating better conditions for the flow of groundwater, and further aggravating the sanding of the dolomite, thus affecting the stability of the surrounding rock of the tunnel.

3.5 Mechanism of microcosmic dissolution of dolomite sanding

Through experimental analysis of the micro characteristics of sandified dolomite, while maintaining the original rock structure, the micro dissolution process of dolomite can be divided into two stages: infiltration dissolution and mechanical disintegration and detachment (Zhang et al., 2012).

(1) Osmotic corrosion stage: water medium penetrates through various primary cracks and interlayer cracks, sutures, structural cracks, micro-cracks and mineral contact sites. This process is mainly based on chemical corrosion, and selective corrosion is often carried out along the crystal surface or intergranular pores, so that some fine cracks or irregular solution pores are distributed on the crystal surface conducive to dissolution. These pores are mostly developed around the intersection of cracks, and the aperture is small, generally 0.001–0.002 mm, and the maximum can reach more than 1mm, and the number varies with the degree of crack development.

(2) Mechanical disintegration and fall off stage: With the further expansion of the dissolution, the dissolution is preferentially strengthened in the channel that is more conducive to the movement of karst water. At this time, water penetrates along the pores between the grains of the rock and the cleavage plane inside the crystals to dissolve around the grains. With the dissolution further along the intergranular pores and the cleavage plane inside the crystal, the dolomite crystal is cut into a network shape, and disintegrates along the internal cleavage plane, weakening the bonding force. With the deepening of the dissolution, the grains are eventually shed into fine particles, forming the violently sanding dolomite sand.

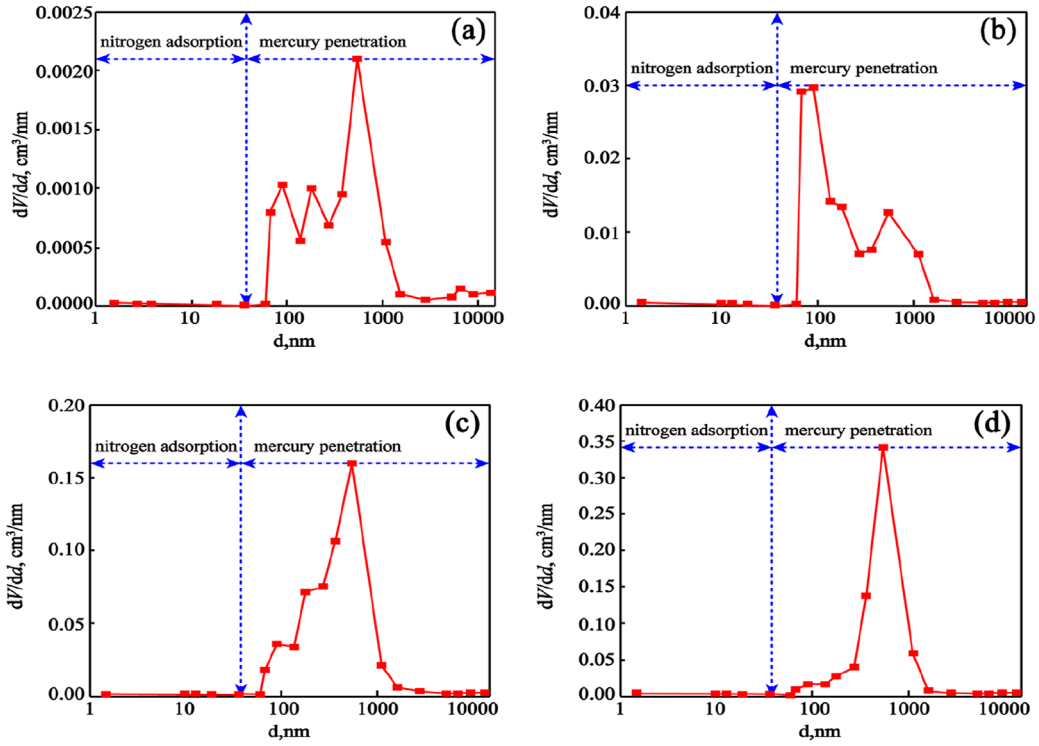

FIGURE 6
Results of pore structure of dolomite with different sanding grades **(a)** slight sanding dolomite, **(b)** moderate sanding dolomite, **(c)** strong sanding dolomite, **(d)** severe sanding dolomite.

Dolomite has a completely different dissolution control mechanism from limestone. Compared with limestone, dolomite has more uniform karst development and water content, and it is difficult to form large pipes and karst caves. The process of dolomite sanding includes chemical dissolution and physical disintegration. Chemical dissolution is the prerequisite for the development of dolomite sanding, and the continuous dissolution expands the transport channel of water medium in dolomite. Physical disintegration is the main material cause of dolomite sand powder, and the interaction and interdependence between the two promote the occurrence and development of karst sanding.

4 Acquisition of mechanical parameters of sanding dolomite

The above studies have been carried out on the sanding grade of dolomite and its microscopic mechanism. However, in actual engineering, how to accurately obtain the physical and mechanical parameters of sanding dolomite is very important for engineering design, calculation and construction. In this study, the wave velocity and integrity coefficient of rock mass were introduced, and the Hoek-Brown strength criterion was modified and improved based on the field needle injection test on the basis of considering the degree of rock mass disturbance, and then the mechanical parameters of sanded dolomite were estimated. Finally, the estimated results were compared with the field adit test results to verify the rationality of the estimated model.

4.1 Revised Hoek-Brown strength criteria

According to the Hoek-Brown strength criteria, there are:

$$\sigma_1 = \sigma_3 + \sigma_{ci}\left(m_b \frac{\sigma_3}{\sigma_{ci}} + \mathrm{s}\right)^a \tag{1}$$

$$m_b = m_i \cdot \exp\left(\frac{GSI - 100}{28 - 14D}\right) \tag{2}$$

$$\boldsymbol{s} = \exp\left(\frac{GSI - 100}{9 - 3D}\right) \tag{3}$$

$$\boldsymbol{a} = 0.5 + \frac{1}{6}\left(e^{\frac{-GSI}{15}} - e^{\frac{-20}{3}}\right) \tag{4}$$

Where σ_1 is the maximum principal stress of rock mass failure; σ_3 is the minimum principal stress of rock mass failure; σ_{ci} is the uniaxial compressive strength of intact rock (It can be measured by the needle penetration test site); m_b is the reduction value of the complete rock empirical parameter m_i; a is the characteristic constant of jointed rock mass; s represents the degree of fracture of rock mass, m_b, a, s are the material parameters of rock mass; GSI is a geological strength index, which is used to estimate the strength of rock mass under different geological conditions; D is the parameter of the disturbed degree of jointed rock mass damage and stress relaxation, the value of which is D = 0–1, and for undisturbed rock mass, D = 0, for severely disturbed rock mass, D = 1.

As can be seen from Formulas 1–4, when determining rock mass mechanical parameters by Hoek-Brown strength criterion, the key is to determine geological strength index GSI and rock

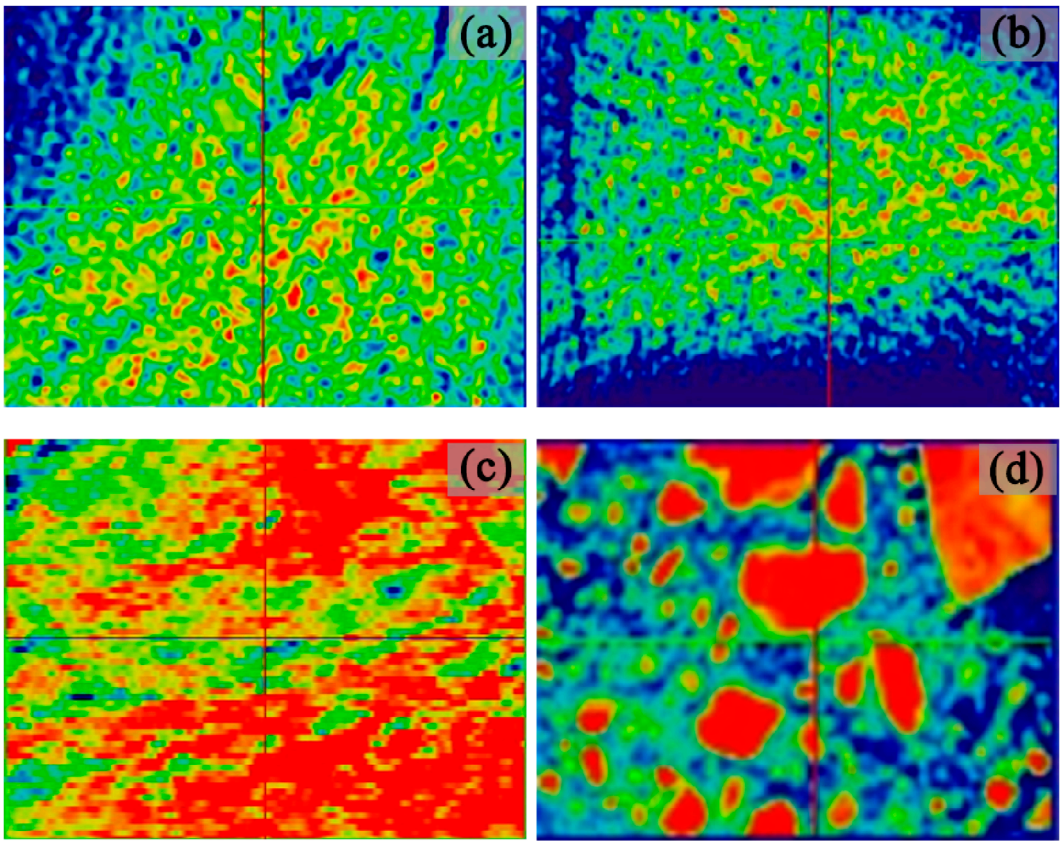

FIGURE 7
CT scan image of pore structure of dolomite with different sanding degrees **(a)** slight sanding dolomite, **(b)** moderate sanding dolomite, **(c)** strong sanding dolomite, **(d)** severe sanding dolomite.

mass disturbance strength *D*. However, when determining these two parameters, Hoek only qualitatively describes the rock mass, and then gives a certain value range based on experience, so the obtained rock mass mechanical parameters have large errors and subjectivity. The wave velocity measurement of rock mass is convenient and the measuring range is controllable. More importantly, the influencing factors of the test results are consistent with the factors considered in the values of geological strength index *GSI* and rock mass disturbance strength *D*.

According to literature (Weng, 1984), the relationship between rock mass disturbance degree D and rock mass wave velocity is as follows:

$$\boldsymbol{D} = 1 - K_v = 1 - \left(\frac{V_p}{V_r}\right)^2 \tag{5}$$

Where K_v is the integrity index of rock mass, V_p is the velocity of sound wave propagation in rock mass, V_r is the speed of sound wave propagation in rock mass.

In the absence of rock wave velocity measurement (Equation 6), it can be estimated according to the statistical formula given by the Southwest Research Institute of the Ministry of Railways:

$$K_v = 1.087 - \frac{J_v}{42.3} \tag{6}$$

Where J_v is the volume joint number of rock mass.

N Barton, through the statistics and summary of a large number of rock engineering data from China, Sweden, Norway and other countries, conclude the relationship between rock mass quality index Q, rock mass wave velocity and rock mass RMR89, as shown in Equations 7, 8:

$$\boldsymbol{Q} = 10^{v_p - 3.5} \tag{7}$$

$$\boldsymbol{RMR}_{89} = 15 \lg Q + 50 \tag{8}$$

According to the relationship between RMR89 classification index value and geological intensity index GSI value:

$$\boldsymbol{GSI} = RMR_{89} - 50, \left(RMR_{89} > 23\right) \tag{9}$$

By bringing Equations 7, 8 into Equation 9, the relationship between geological strength index GSI value and rock wave velocity can be obtained:

$$\boldsymbol{GSI} = 15V_p - 7.5 \tag{10}$$

By bringing Equations 5, 10 into Equations 2–4, m_b, s and a based on rock mass wave velocity of Equations 11–13 can be obtained Vp:

$$m_b = m_i \cdot \exp\left(\frac{15V_p - 107.5}{14 + 14\left(\frac{V_p}{V_r}\right)^2}\right) \tag{11}$$

TABLE 5 Mechanical parameters of dolomite rock mass estimated by generalized Hoek-Brown criterion.

degree of sanding	V_p (m·s^{-1})	c' (MPa)	φ' (°)	E_m (GPa)
severe sanding	1720–1820 (1765)	0.29~0.25 (0.22)	28.04~33.55 (30.72)	0.63~0.87 (0.74)
strong sanding	3,130–3,900 (3,340)	0.34~0.71 (0.44)	38.59~50.96 (43.02)	1.15~2.61 (1.58)

$$s = \exp\left(\frac{15V_p - 107.5}{3\left(\frac{V_p}{V_r}\right)^2 + 6}\right) \tag{12}$$

$$a = 0.5 + \frac{1}{6}\left(e^{\frac{1-2V_p}{2}} - e^{\frac{-20}{3}}\right) \tag{13}$$

The calculation formula of rock mass deformation modulus determined by rock mass wave velocity is obtained as Equation 14:

When $\sigma_{ci} \leq 100$ MPa,

$$E_m = \frac{1}{2}\left[1 + \left(\frac{V_p}{V_r}\right)^2\right]\sqrt{\frac{\sigma_{ci}}{100}} \times 10^{\frac{15V_p - 17.5}{40}} \tag{14}$$

When $\sigma_{ci} > 100$ MPa,

$$E_m = \frac{1}{2}\left[1 + \left(\frac{V_p}{V_r}\right)^2\right] \times 10^{\frac{15V_p - 17.5}{40}}$$

Where E_m is the deformation modulus of rock mass.

According to the conversion formula of Mohr-Coulomb criterion and Hoek-Brown strength criterion, the shear strength parameters of rock mass are obtained as Equations 15, 16:

$$\varphi' = \sin^{-1}\left[\frac{6am_b(s + m_b\sigma_{3n})^{a-1}}{2(1+a)(2+a) + 6am_b(s + m_b\sigma_{3n})^{a-1}}\right] \tag{15}$$

$$c' = \frac{\sigma_{ci}[(1+2a)s + (1-a)m_b\sigma_{3n}](s + m_b\sigma_{3n})^{a-1}}{(1+a)(2+a)\sqrt{1 + 6am_b(s + m_b\sigma_{3n})^{a-1}/(1+a)(2+a)}} \tag{16}$$

Where φ' is the internal friction Angle, c' is the stands for cohesion, σ_{3n} is the upper limit of lateral stress.

4.2 Analysis of estimated results

The dolomite with strong sanding and severe sanding near the 2# branch hole of XiaoPu Tunnel in Yuxi Section of Central Yunnan Water diversion Project was taken as an example to estimate, and the needle penetration test with SH-70 needle penetration instrument produced by Maruto Company of Japan and the field adit test were carried out. The mechanical parameters of strong and severe sanding dolomite rock mass estimated based on the generalized Hoek-Brown strength criterion were shown in Table 5. The mechanical parameters of strong and severe sanding dolomite rock mass estimated according to the field needle penetration test and the empirical model of to needle penetration ratio (NPI-c) and internal friction Angle to needle penetration ratio (NPI-φ) are shown in Table 6. The mechanical parameters of rock mass obtained by direct shear test and deformation test in the field adit of the strong sanding dolomite in Yuxi section are shown in Table 7.

The above are the mechanical parameter results of the strong and severe sanding dolomite rock mass estimated based on the generalized Hoek-Brown strength criterion, and the mechanical parameter results of the rock mass obtained according to the field needle penetration test and field adit test. Figures 8, 9 are the results of further visualization. Compared with the estimated values of cohesive force and internal friction Angle of the severe sanding dolomite in Figures 8A, B, it can be seen that the cohesive force estimated by the generalized H-B criterion is 0.25~0.29 MPa, and the internal friction Angle is 28.04~33.55°. The cohesive force c estimated by NPI is 0.086~0.17MPa, and the internal friction Angle is 16.17~19.08. The cohesive force and internal friction Angle estimated by generalized H-B criterion are both higher than those estimated by NPI. However, the values of c and φ estimated by NPI are closer to the recommended values of c (0.05~0.07) and φ (16.7~21.8) given by the design unit.

Figure 9 shows the comparis on of mechanical parameters of strong sanding dolomite rock mass. The cohesive force estimated by generalized H-B criterion is 0.34–0.71 MPa, the cohesive force estimated by NPI is 0.30~1.60 MPa, and the cohesive force obtained by field direct shear test is 0.14~0.413 MPa. Compared with the estimated value of NPI, the cohesive force value estimated by the generalized H-B criterion is more concentrated, but most of the data points estimated by the two methods are close to the median value of 0.308 MPa which is obtained in the direct shear test and some of the cohesive force value estimated by NPI is 0.308 MPa. As shown in Figure 9B, the internal friction Angle estimated by the generalized H-B criterion is 38.59~50.96°, the internal friction Angle estimated by NPI is 22.13~33.64°, and the internal friction Angle obtained by the field direct shear test is 27.92~33.82°. Compared with each other, the internal friction Angle estimated by the generalized H-B criterion is the largest, and the values are not in the range of the rock mass direct shear test, while some of the data points estimated by NPI fall within the range of the rock mass direct shear test. As shown in Figure 9C, the deformation modulus of strong sanding dolomite estimated based on the generalized H-B criterion is basically located in the range of value of the adit deformation test, mainly concentrated in the range of 1.15–1.6GPa, and is significantly higher than the deformation modulus of strong sanding dolomite.

Therefore, the estimation of mechanical parameters of rock mass based on generalized H-B criterion and NPI can be used for reference. In order to quickly obtain mechanical parameters of strong and severe sandin dolomite in the field, the estimation method based on generalized H-B criterion and the injection penetration test can be considered as a quick and economic means.

TABLE 6 Mechanical parameters of dolomitic rock mass estimated by needle penetration tesx

degree of sanding	Needle penetration index (N/mm)	c (MPa)	φ (°)	Uniaxial compressive strength (MPa)
severe sanding	0.70~4.13 (2.10)	0.086~0.17 (0.12)	16.17~19.08 (17.56)	0.88~1.67 (1.23)
strong sanding	7.5~40 (15.11)	0.30~1.60 (0.604)	22.13~33.64 (25.78)	3.00~15.41 (5.93)

Note: values in brackets are the average values of data.

TABLE 7 Results of adit test of strong sanding dolomitein in Yuxi section.

Adit number	degree of sanding	Direct shear test		Deformation test	
		c' (MPa)	φ' (°)	Modulus of deformation (GPa)	Elasticity modulus (GPa)
XQPD-103	strong sanding	0.140	27.92	1.24	2.69
XQPD-104		0.413	33.82	1.75	2.93
XQPD-105		0.372	31.80	0.875	1.871
average value		0.308	31.18	1.619	2.783

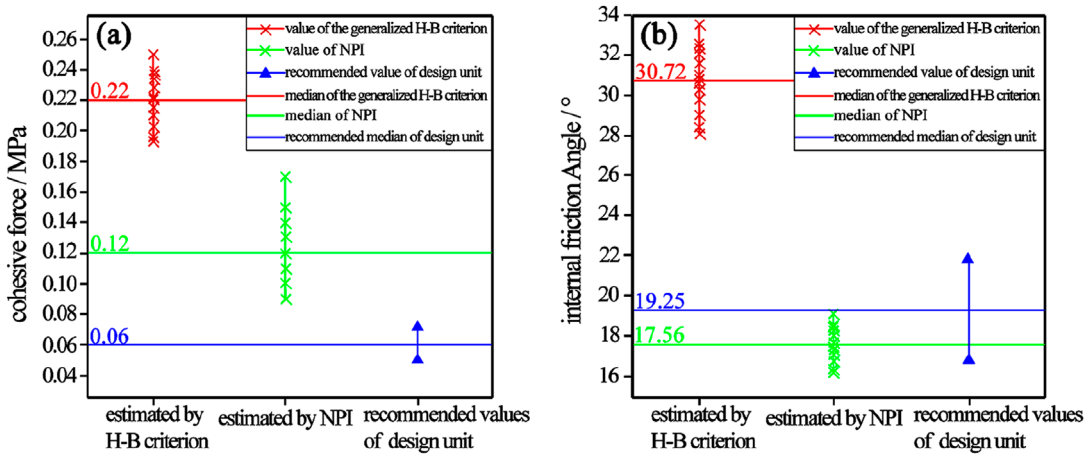

FIGURE 8
Comparison of estimated values of cohesive force and internal friction angle of severe sanding dolomite under different methods **(a)** comparison of cohesion, **(b)** comparison of internal friction angles.

5 Discussion

The study studies the special engineering geological characteristics of sanding dolomite by various means. Although some researches on sandification of dolomite have been carried out in the existing literature, most of the researches remain in the description and theoretical analysis of macro phenomena, and the researches on the microstructure of dolomite with different degrees of sandification are relatively lacking. Meanwhile, the difficulty of making standard rock samples for laboratory tests to obtain rock mechanics parameters has not been solved in view of the structure fragmentation and joint development of dolomitization rock mass. In this paper, the classification standard of sanding dolomite is given, the microstructure and mechanism of dolomite with different degree of sandification are studied in detail, and the estimation method of mechanical parameters of sanding dolomite is proposed. At the same time, the mechanical parameters of sanding dolomite can be obtained quickly without complicated laboratory tests.However, in this paper, only the microstructure and mechanism of sanding dolomite have been analyzed, and the influence on macro environment, medium conditions and regional structure has not been analyzed, which needs to be further

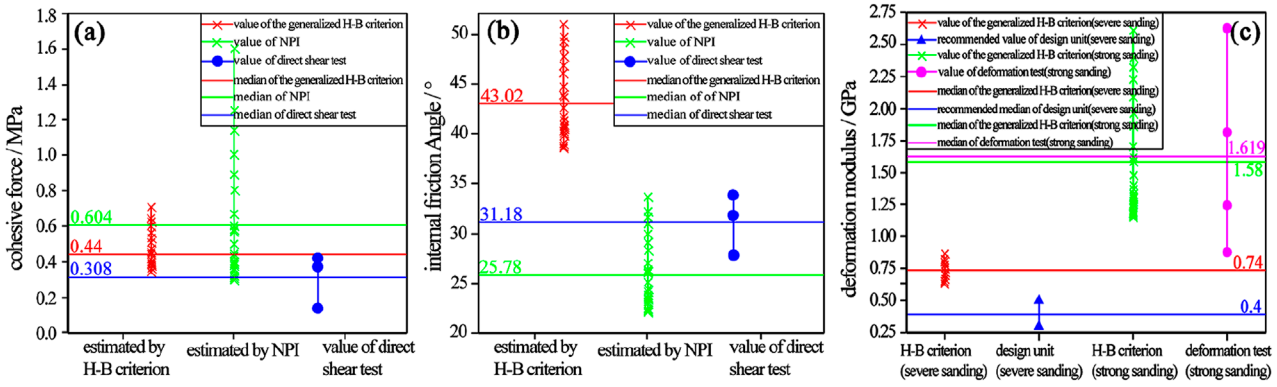

FIGURE 9
Comparison of estimated values of mechanical parameter of strong sanding dolomite under different methods **(a)** comparison of cohesion, **(b)** comparison of internal friction angles, **(c)** comparison of deformation modulus.

studied. In addition, although the indexes for the classification of sandification of dolomite grades are given in this paper, due to the large uncertainty of the geological environment, it is better to consider some field descriptions and field experience when determining the sandification of dolomite grades.

6 Conclusion

Based on the background of the sanding dolomite tunnel in Yuxi Section of the Central Yunnan water diversion Project, this study introduced analytic hierarchy process and fuzzy comprehensive evaluation method to classify the dolomite sanding grade, and carried out SEM and CT scanning tests for different sanding dolomite degrees to study the microscopic composition and structure of the dolomite. Based on the Hoek-Brown strength criterion considering rock wave velocity and integrity coefficient, an estimation method of mechanical parameters of sanding dolomite was proposed and verified. The main conclusions are as follows:

(1) The sanding dolomite was divided into four grades: slight sanding dolomite, moderate sanding dolomite, strong sanding dolomite and severe sanding dolomite by 15 main indexes selected from three aspects: external characteristics, structural characteristics and physical and mechanical indexes. The evaluation standard value of each evaluation index and its weight coefficient in the classification of sanding grade were summarized.

(2) According to the comprehensive analysis of the detection results of SEM and CT, with the increase of dolomite sanding grade, the more intense the development of void and fracture of dolomite, the lower the interaction force between rock masses and the lower the mechanical strength of rock mass, which affects the stability of surrounding rock of the tunnel. The action of groundwater will intensify the dolomite dissolution and sanding, leading to the fracture of surrounding rock. The degree of pore development from high to low is in order of intense sanded dolomite, strong sanded dolomite, medium sanded dolomite and micro-new rock mass.

(3) The Hoek-Brown strength criterion was modified and improved by introducing rock wave velocity and rock integrity coefficient, and a method for estimating mechanical parameters of sanding dolomite was proposed. The estimated cohesion of strong sanding dolomite is 0.34~0.71 MPa, the internal friction Angle is 38.59~50.96°, the uniaxial compressive strength is 3~15.41 MPa, the estimated cohesion of severe sanding dolomite is 0.086~0.17 MPa, the internal friction Angle is 16.17~19.08°, and the uniaxial compressive strength is 0.88–1.67 MPa.

(4) By comparing and analyzing the mechanical parameters of rock mass obtained by Hoek-Beown strength criterion method, NPI estimation method and *in-situ* rock mass tunnel test method, the results show that Hoek-Beown strength criterion has good applicability in the estimation of mechanical parameters of sanded dolomite rock mass, and this method can be used to estimate the mechanical parameters of sanded dolomite. At the same time, NPI estimation method can be used to quickly obtain mechanical parameters of sanded dolomite in the field.

(5) The research results will help engineers and scholars to better understand the geological characteristics of sanding dolomite, which is helpful to carry out engineering construction in sanded dolomite areas.

Data availability statement

The original contributions presented in the study are included in the article/supplementary material, further inquiries can be directed to the corresponding author.

Author contributions

FW: Writing–original draft. ZL: Writing–review and editing. YS: Conceptualization, Writing–review and editing. XG: Data curation, Writing–review and editing. YZ: Resources, Writing–review and editing.

Funding

The author(s) declare that financial support was received for the research, authorship, and/or publication of this article. This research was funded by National Natural Science Foundation of China - Railway Fundamental Research Joint Fund Project (U2468219), Shanxi Province Basic Research Program (202303021212371), Applied Basic Research Project of Shanxi Communications Holding Group (2022-JKKJ-6).

Acknowledgments

The experimental data and photographs in this study were provided to the authors through the efforts of all participants in the model experiment.

Conflict of interest

Authors FW, ZL, and YS were employed by Shanxi Traffic Technology Research and Development Co., LTD. Authors FW, ZL, and YS were employed by Shanxi Intelligent Transportation Laboratory Co., LTD. Authors XG and YZ were employed by Yunnan Dianzhong Water Diversion Engineering Co., LTD.

Generative AI statement

The author(s) declare that no Generative AI was used in the creation of this manuscript.

Publisher's note

All claims expressed in this article are solely those of the authors and do not necessarily represent those of their affiliated organizations, or those of the publisher, the editors and the reviewers. Any product that may be evaluated in this article, or claim that may be made by its manufacturer, is not guaranteed or endorsed by the publisher.

Author disclaimer

Any views and opinions expressed in the study were those of the authors.

References

Chen, W., Wan, W., and Feng, T. (2022). Dolomite 'smacro-microscopic mechanism of mechanical property deterioration under high-humidity conditions. *J. China Coal Soc.* 47 (11), 4023–4039.

Cui, Q. L., Wu, H. N., Shen, S. L., Xu, Y. S., and Ye, G. L. (2015). Chinese Karst geology and measures to prevent geohazards during shield tunnelling in karst region with caves. *Nat. Hazards* 1 (77), 129–152. doi:10.1007/s11069-014-1585-6

Dong, J. X., Shen, Z. L., Cao, L., Mi, J., Li, J. g., Zhao, Y. c., et al. (2023). Water-sand inrush risk assessment method of sandy dolomite tunnel and its application in the Chenaju tunnel, southwest of China. *Geomatics, Nat. Hazards Risk* 14 (01), 2196369. doi:10.1080/19475705.2023.2196369

Dong, J. X., Zhou, Z. Q., Wang, Z. R., Zhao, Y. R., Li, J. G., Mu, C. Y., et al. (2022). Estimation of mechanical parameters of intensively sandy dolomite based on Hoek-Brown strength criterion. *J. Changjiang River Sci. Res. Inst.* 39 (12), 21–25.

Dong, J. X., Yang, J., Zhou, L. S., Mi, J., Zhou, Y. J., Li, J. G., et al. (2024). Study on disaster-causing structure classification, disaster-pregnant and failure modes of surrounding rock mass in sandy dolomite tunnels. *Chinese Journal of Rock Mechanics and Engineering* 43 (5), 1064–1079.

Guo, J. Q., Liu, X. L., and Qiao, C. S. (2014). Experimental study of mechanical properties and energy mechanism of Karst limestone under natural and saturated states. *Chin. J. Rock Mech. Eng.* 33 (02), 296–308.

Jiang, Y. F., Zhou, F. C., Lin, J. Y., Li, J., Qi, Y., Li, X., et al. (2023). Evolution mechanism of tunnel water and sand inrush considering water-rich sandy dolomite hazard-causing structures. *Eng. Fail. Anal.* 153, 107554. doi:10.1016/j.engfailanal.2023.107554

Li, S. C., Xu, Z. H., Huang, X., Lin, P., Zhao, X. C., Zhang, Q. S., et al. (2018). Classification, geological identification, hazard mode and typical case studies f hazard-causing structures for water and mud inrush in tunnels. *Chin. J. Rock Mech. Eng.* 5 (37), 1041–1069.

Liu, X. Y., Hu, K. F., Zhang, W. T., Shi, J. F., Wan, Y., and Zhou, Y. Z. (2022). Study on the treatment of water gusher and mud in dolomite sanded tunnel of central Yunnan Water diversion Project. *Yangtze River* 53 (9), 102–108.

Masaharu, F., Shin-Ichi, O., and Yoshio, S. (2011). Cementation of sands due to microbiologically-induced carbonate precipitation. *Soils Found.* 1 (51), 83–93.

Richter, D. K., Gillhaus, A., and Neuser, R. D.(2018). The alteration and disintegration of dolostones with stoichiometric dolomite crystals to dolomite sand: new insights from the Franconian Alb. *Z. Dtsch. Ges. für Geowiss.* 1(169), 27–46.

Sajjad, M., Mohammad, R., Hosseinzadeh, D. R., and Choulet, F. (2020). Geological and geochemical constraints on the Farahabad vent-proximal sub-seafloor replacement SEDEX-type deposit, Southern Yazd basin, Iran. *J. Geochem. Explor.* 209, 106436. doi:10.1016/j.gexplo.2019.106436

Tian, Q. W., and Yue, C. L. (2014). Characteristics of karst sanded fine-crystalline dolomite and wall rock classification for Pingtou Hydropower Station. *Advan. Sci. Techn. Water. Res.* 34 (5), 45–49.

Wang, F., Zhao, Y., Li, C., Li, C., Lan, T., Ping, S., et al. (2019). An experimental study on the corrosion characteristics of the karst tunnel engineering area in Southwest China. *Bull. Eng. Geol. Environ.* 6 (78), 4047–4061. doi:10.1007/s10064-018-1411-6

Wang, Z. J., Du, Y. W., Jiang, Y. F., Wu, F., Qi, Y. L., and Zhou, P. (2021). Study on the mechanism of instability of tunnel face in sandy dolomite stratum. *Chin. J. Rock Mech. Eng.* 11 (40), 3118–3126.

Weng, J. T. (1984). Differential dissolution of calcite and dolomite. *Karst China* 1984 (1), 29–37.

Wu, F. (2021). *Study on the disaster mechanism of the tunnel in the water-rich sanded dolomite strata*. (master's thesis.) Southwest Jiaotong University.

Wu, G. J., Chen, W. Z., Yuan, J. Q., Yang, D. s., and Bian, H. b. (2017). Formation mechanisms of water inrush and mud burst in a migmatite tunnel: a case study in China. *J. Mt. Sci.* 1 (14), 188–195. doi:10.1007/s11629-016-4070-8

Wu, J. Y., Jing, H. W., Gao, Y., Meng, Q., Yin, Q., and Du, Y. (2022). Effects of carbon nanotube dosage and aggregate size distribution on mechanical property and microstructure of cemented rockfill. *Cem. Concr. Compos.* 127, 104408. doi:10.1016/j.cemconcomp.2022.104408

Wu, J. Y., Jing, H. W., Yin, Q., Yu, L., Meng, B., and Li, S. (2020). Strength prediction model considering material, ultrasonic and stress of cemented waste rock backfill for recycling gangue. *J. Clean. Prod.* 276, 123189. doi:10.1016/j.jclepro.2020.123189

Wu, J. Y., Wong, H. S., Zhang, H., Yin, Q., Jing, H., and Ma, D. (2024). Improvement of cemented rockfill by premixing low-alkalinity activator and fly ash for recycling gangue and partially replacing cement. *Cem. Concr. Compos.* 145, 105345. doi:10.1016/j.cemconcomp.2023.105345

Wu, W. L., Liu, X. L., Guo, J. Q., Sun, F., Huang, X., and Zhu, Z. (2021). Upper limit analysis of stability of the water-resistant rock mass of a Karst tunnel face considering the seepage force. *Bull. Eng. Geol. Environ.* 7 (80), 5813–5830. doi:10.1007/s10064-021-02283-6

Yan, Z. W., Zhang, J. F., Huang, S. J., and Wang, H. J. (2007). Characteristics and origin of interlayer dissolution residual deposits in Dongxiang copper mine, Jiangxi Province. *Karst China* 26 (2), 126–131.

Yang, W. M., Yang, X., Fang, Z. D., Shi, S., Wang, H., Bu, L., et al. (2019). Model test for water inrush caused by Karst caves filled with confined water in tunnels. *Arabian J. Geosciences* 24 (12), 749. doi:10.1007/s12517-019-4907-x

Yin, Q., Nie, X. X., Wu, J. Y., Wang, Q., Bian, K., Jing, H., et al. (2023a). *Experimental study on unloading induced shear performances of 3D saw-tooth rock fractures*.

Yin, Q., Zhu, C., Wu, J. Y., Pu, H., Wang, Q., Zhang, Y., et al. (2023b). Shear sliding of rough-walled fracture surfaces under unloading normal stress. *J. Rock Mech. Geotechnical Eng.* 15 (10), 2658–2675. doi:10.1016/j.jrmge.2023.02.005

Zhang, H. Q., Zhao, Q. H., and Peng, S. Q. (2012). Rock mass quality classification and deep Karst sandification of dolomite about Pingtou hydroelectric station at the Meigu river. *China Rural Water Hydropower* 2012 (7), 151–155.

Zhang, Z. M. (2025). Analysis on the application of In-situ testing technology in geotechnical engineering geological investigation. *J. Eng. Technol. Res.* 10 (1), 223–225. doi:10.19537/j.cnki.2096-2789.2025.02.073

Zhang, L. X., Zhao, Q. H., Hu, X. B., Han, G., and Zhao, X. (2012). Laboratory dissolution test on dolomite and its micro dissolution mechanism. *J. Eng. Geol.* 20 (4), 556–584.

Zhao, Y. R. (2021). *Study on physical and mechanical properties of intensely sanded dolomite in central Yunnan water diversion Project*. (master's thesis.) Kunming University of Science and Technology.

Zhou, P., Jiang, Y., Zhou, F., Wu, F., Qi, Y., and Wang, Z. (2022). Disaster mechanism of tunnel face with large section in sandy dolomite stratum. *Eng. Fail. Anal.* 131, 105905. doi:10.1016/j.engfailanal.2021.105905

Zhu, Q., Yin, Q., Tao, Z. G., Yin, Z. Q., Jing, H.W., Meng, B., et al. (2024). Shearing characteristics and instability mechanisms of rough rock joints under cyclic normal loading conditions. *J. Rock Mech. Geotechnical Eng.* 05 (49). doi:10.1016/j.jrmge.2024.05.049

Zhu, Q., Yin, Q., Tao, Z. G., Wu, J. Y., He, M., Zha, W., et al. (2024a). Cyclic frictional response of rough rock joints under shear disturbances: laboratory experiment and numerical simulation. *Eng. Fract. Mech.* 310, 110514. doi:10.1016/j.engfracmech.2024.110514